LBL-7432
UC-4
TID-4500-R66

RADIATION CHEMISTRY OF PARTICLES ACCELERATED BY THE BEVALAC

M. Jayko, A. Appleby, E. Christman,
A. Chatterjee, and J. Magee

DONNER LABORATORY

April 1978

Prepared for the U. S. Department of Energy
under Contract W-7405-ENG-48

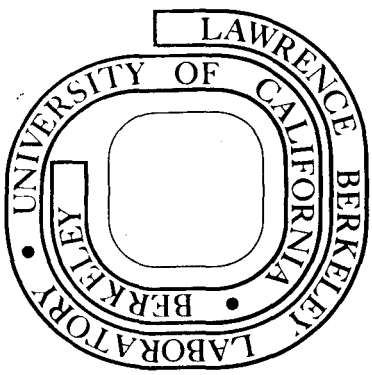

DISCLAIMER

RADIATION CHEMISTRY OF PARTICLES ACCELERATED BY THE BEVALAC

M. Jayko*, A. Appleby§, E. Christman§, A. Chatterjee†, and J. Magee†

*Materials and Molecular Research Division
†Biology and Medicine Division
Lawrence Berkeley Laboratory
University of California

§ Environmental Science Department
Rutgers University

INTRODUCTION

As a part of a program to determine the physical, chemical, and biological properties of accelerated heavy particles, the radiation chemistry of aqueous systems under irradiation with carbon, neon, and argon beams from the Bevalac has been investigated. Preliminary reports on this work have been presented (1,2,3). The systems for study were chosen with two considerations in mind: (a) to make the widest possible comparison with well-established results of radiation chemistry, and (b) to collect basic data for the elucidation of the properties of heavy-particle tracks.

The first consideration led to the selection of the acid ferrous sulfate system. This system has been studied extensively using radiation of varied qualities and is one of the best understood of all the aqueous systems. It is known as the "Fricke dosimeter" and is widely used in radiation biology.

The second consideration led to a selection of additional reactions that would allow a determination of the "primary products" of the heavy-particle irradiations. According to radiation chemical theory, the initial chemical

products in an irradiated aqueous system are hydrated electrons (e^-_{aq}), H atoms, OH radicals, and H_3O^+ ions produced in the particle tracks. These intermediates are created in high concentrations and as they diffuse away from the tracks they react with each other and with any other reactive material present. H atoms reacting together produce H_2 molecules; the reaction of OH radicals produce H_2O_2 molecules. H_2 and H_2O_2 molecules released from the tracks into the solution are called "primary molecular" products. Similarly, the radicals that escape combination in the tracks and diffuse into the solution are called "primary radical" products. The molecular and radical product yields are very important; they depend on the particle, its LET, charge, etc.

This brief sketch of the theory of the radiation chemistry of water suggests several lines of experimentation to obtain basic chemical data on heavy particles. The "molecular" and "radical" yields depend on the concentrations of added chemicals (usually called scavengers). The simplest explanation for the dependence of primary yields on scavenger concentrations is in terms of the initial distributions in space--and hence the initial concentrations in the tracks. Thus, variation of the primary yields with scavenger concentration can be related to track structure. The time dependence of the radical reactions is determined by scavenger concentration in addition to diffusion coefficients, reaction rate constants, and initial radical concentrations. A complete set of track studies would require time resolution of the radical reactions in systems of various scavenger concentrations. Such investigations are planned.

It is usually assumed that the initial yields of e^-_{aq}, H, OH, and H_3O^+ are independent of LET, and that excited electronic states are not important. The validity of these assumptions should be investigated over the wide range

of properties available with Bevalac particles, and experiments are now being designed for this purpose. Under conditions of the smallest energy density of deposit by particles (for example below 1 eV/Å) it is reasonable to assume the initial products are always the same. On the other hand, high Z particles with small track volumes can deposit 10^2 to 10^3 eV/Å and are presumed to produce additional effects. Such effects are of interest to the physics, chemistry, and biology of accelerated particles, but no explicit consideration of them is made here.

EXPERIMENTAL

The chemical systems were irradiated in cells designed to provide an optimum condition for product formation, i.e., to obtain easily measurable yields in the shortest irradiation time. Irradiation cells 3.2 cm in diameter and 1-cm thick with a volume of 8.3 ml were selected. These cells provide sufficient solution for optical measurement, and the Bevalac beam can be focused and centered on the target so that an acceptably small fraction of the volume is outside of the irradiated region. Usually 75% of the beam is within a circle 1 cm in diameter. The cells are made of quartz with windows ranging from 1.65- to 1.80-mm thick and parallel to within 0.025 mm. They were fitted with necks 10 to 12-cm long with ground glass stoppers. The arrangement for the irradiation is shown in Figure 1. The irradiation cells were used in sets which were matched according to window thickness so that several sets could be used interchangeably and still have the same total window thickness.

Two techniques were used to irradiate the cells simultaneously: (a) the entire Bragg curve was measured (which in the case of 400 Mev/n carbon

would require sixteen cells), or (b) the variable water column was used to degrade the beam before it entered the first cell. Most often the water column was adjusted so that in a set of eight cells, the Bragg peak was 1 to 2 mm in front of the downstream window of cell number six. At first the actual location of the Bragg peak was determined experimentally. However, the position was subsequently calculated by considering the density of the target solution and using the factor 1.838 to compare the relative stopping power of water and quartz. In this manner, the Bragg peak can be placed at any desired position to ±0.5 mm. The location of the Bragg peak with respect to the sample cell is shown in Figure 2. (The four cells whose positions are noted in Figure 2 are reported on here. Dosimetry at the Bragg peak is less certain for the reasons discussed in the text and will be reported on at a later date.) Since collimators were not used, polaroid film was used to verify the correct alignment of the cells, and to provide a permanent record of the size and shape of the beam.

The measurement of the energy absorbed in the target cells and the basis for calculation of G values is dependent on the ion chambers. The energy at the point of extraction is determined from relationships between radio frequency, the radius of extraction, and magnetic field strength. The incident beam energy at the target can be determined by the relationship between range and energy as evaluated by Northcliffe (4). Ions collected are determined by total charge and average charge, with an error of ±3%. Two assumptions have been made that affect the calculation of absolute G values and they both have to do with the ion chamber. First, the W value assumed for heavy ions in nitrogen gas is 34.9 eV per ion pair; second, the relative mass stopping power of water to nitrogen is assumed to be 1.125.

At present the uncertainties in G values are greater than ±5%. The greatest contribution to this rather large uncertainty is the lack of quantitative knowledge of the process of nuclear fragmentation of the incident beam. Qualitatively, we know that nuclear fragmentation alters G values, in the direction of lower LET.

Currently it is not possible to extract beams at lower energies from the Bevalac; hence, the most practical way to reduce the beam energy is to use a water column. This introduces beam fragmentation that results in uncertainties. Even without this water column, we are not free from nuclear fragmentation because of the presence of beam monitoring devices. For example, before the beam even gets to the first ion chamber it has penetrated 2 gm/cm^2 of absorbing materials.

The range and shape of the Bragg curves may change under actual experimental conditions. These variations must be carefully evaluated because the dose we calculate for each cell is a product of the entrance dose and the relative ionization at the point in the Bragg curve corresponding to the location of the cell of interest. Obviously, this problem is magnified both at and near the Bragg peak.

Ferric yields from the Fricke dosimeter were measured within five minutes of the irradiation using a Beckman DU spectrophotometer. The optical density was measured at 304 nm using 1-cm cells. The extinction coefficient used was ϵ = 2170 at 25^{o} C. Sulfuric acid (0.8 N) was used with sodium chloride (10^{-3} M) to inhibit interference from any possible organic impurity present. All targets were made up in triple distilled water. Deionized water was distilled from alkaline permanganate and then from phosphoric acid. In the

oxygen free system, oxygen was removed by bubbling with nitrogen using a manifold which could degas the entire set of cells simultaneously.

Hydrogen peroxide produced in the sodium bromide and sodium formate systems were measured following the irradiation (5,6) using the method of A. Ghormley. Samples were stored and transported in poly-stoppered glass vials, and the analysis in all cases was completed within twelve hours of irradiation. Nitrite determinations were measured according to the method of Rider and Mellon (7).

Whenever possible, the dose rate was kept in the range of 2000 to 3000 rad per minute as measured on the 3-cm ring of the ion chamber. There are approximately fifteen 500 millisec pulses per minute. Total doses were in the range of 2 to 20 kilorad depending on the requirements of the chemical system used.

The results obtained from experiments described in this report must be considered preliminary. The uncertainties (particularly in dosimetry) will take additional statistical and theoretical analysis before absolute G values can be reported. Some of the results may be better understood after various chemical, optical, and electronic artifacts have been eliminated.

THE SYSTEMS STUDIED

We have so far studied five different systems (Table 1) for each of the three particles--carbon, neon, and argon. The systems were chosen for two reasons: (a) their radiation chemical response to gamma or x rays is quite well understood, and (b) one can derive the relationships between the observed product yields and the so-called primary yields of molecular and radical products which are present about 100 nanoseconds after the initial energy deposition.

Table 1. Systems Studied

$FeSO_4$ (10^{-2}M) / H_2SO_4 (0.4 M) / air
$FeSO_4$ (10^{-2}M) / H_2SO_4 (0.4 M) / N_2
HCOONa (5×10^{-3} M) / air
NaBr (10^{-3} M) / air
C_2H_5OH (0.025 M) / $NaNO_3$ (0.0025 M) / N_2

The first two systems (ferrous sulfate at 10^{-2} M in 0.4 M sulfuric acid, with and without air present) are at a low pH. They have been extensively studied using protons and deuterons of up to a few tens of MeV, notably by Schuler and Allen (8), and by Hart (9). The reaction mechanisms are well established (10) and the ferric oxidation yields (expressed in molecules per 100 eV deposited) are related to the primary H_2O_2, OH, H, and hydrated electron yields as shown in equations (1) and (2).

$$G(Fe^{3+})_{O_2} = 2G^a_{H_2O_2} + G^a_{OH} + 3G^a_H + 3G^a_{e^-_{aq}} \quad (1)$$

$$G(Fe^{3+})_{N_2} = 2G^a_{H_2O_2} + G^a_{OH} + G^a_H + G_{e^-_{aq}} \quad (2)$$

The yields are somewhat pH dependent so the superscript "a" indicates that these are the values in acid. The total reducing radical yield and the yield of water decomposition (in acid) may be derived from the following equations.

$$G^a_H + G^a_{e^-_{aq}} = \frac{1}{2}\left[G(Fe^{3+})_{O_2} - G(Fe^{3+})_{N_2}\right] \quad (3)$$

$$G^a_{-H_2O} = 2G^a_{H_2O_2} + G^a_{OH} = \frac{1}{2}\left[3G(Fe^{3+})_{N_2} - G(Fe^{3+})_{O_2}\right] \quad (4)$$

The remaining systems are carried out in neutral solutions.

In aerated sodium formate, the hydrogen peroxide measured is generated by the combination of primary yields shown in equation (5).

$$G(H_2O_2)_{HCOO^-} = G_{H_2O_2} + \frac{1}{2}\,G_{OH} + \frac{1}{2}\,G_{e^-_{aq}} + \frac{1}{2}\,G_H \quad (5)$$

In aerated sodium bromide, the OH radical reacts differently (11) and essentially decreases the H_2O_2 yield by one-half equivalent.

$$G(H_2O_2)_{Br^-} = G_{H_2O_2} - \frac{1}{2}\,G_{OH} + \frac{1}{2}\,G_H + \frac{1}{2}\,G_{e^-_{aq}} \quad (6)$$

Thus, the difference between the observed yields of the formate and the bromide systems is equal to the yield of the OH radical.

$$G_{OH} = G(H_2O_2)_{HCOO^-} - G(H_2O_2)_{Br^-} \quad (7)$$

In de-aerated ethanol/nitrate solutions, the hydrated electrons react with the nitrate anion giving an intermediate which converts to nitrite.

There are competitive reactions and only a fraction "f" is measured as nitrite (12).

$$G(NO_2^-) = f\, G_{e^-_{aq}} \qquad (8)$$

The factor "f" depends on the concentrations of ethanol and nitrate. The concentrations used here were chosen so that f = 0.98 and the nitrite yield is essentially equal to the hydrated electron yield.

To summarize, using the systems so far studied we can derive the OH and hydrated electron yields in neutral solution, and the reducing radical and water decomposition yields in acidic solution.

EXPERIMENTAL RESULTS AND DISCUSSION

Figure 3 shows the preliminary results for the two ferrous sulfate systems. The yields are plotted against the mean ion energy for each of the 1-cm sample cells. The G values are calculated from the slopes of linear plots of chemical yield versus dose, each plot having at least four data points. Between two and six replicate runs were made and the present data are their averages. The error bars represent one standard deviation on the average of the runs. The location of the sample cells is shown in Figure 2. (Additional cells further up the plateau were used in some of the runs.) Data from the cells at and beyond the Bragg peak are not included; in these cells the ions are coming to rest, therefore the chemical yields are integral values including contributions from a wide energy range, as well as from a distribution of secondary particles arising from fragmentation. Dosimetry under these circumstances will be uncertain until the distribution of primary and secondary particles is worked out.

It should be noted that for all the ions the ferric yields decrease slightly as the beam energy decreases, and there is a definite reduction in the yield as Z increases. This is seen in the H_2O_2 yields shown in Figure 4. The H_2O_2 yield from aerated bromide is much less dependent on these factors, and indeed the yield for argon seems to increase slightly with beam penetration. The yields from neon and argon are significantly higher than those from carbon. This is qualitatively expected because the H_2O_2 produced in the bromide is much more dominated by the molecular H_2O_2 yield. Earlier work with protons, deuterons, and helium ions has shown that the molecular H_2O_2 yield is much less dependent on ionization density than the radical yields, and that it increases slightly with ionization density.

The nitrite yields from the oxygen free ethanol/nitrate solutions are shown in Figure 5. The same slight decrease with beam penetration and more pronounced decrease with increasing Z can be seen. These G values give the yields of hydrated electrons.

From these data we can derive some individual primary yields (or combinations of them). Figure 6 shows the quantity calculated in equation (3). According to classical radiation chemistry this quantity equals the yield of reducing free radicals that escape the spurs. The thick lines are from the experimental values; the thin lines represent a confidence interval of one standard deviation (±5 to 7%). Clearly these radical yields decrease as the Z increases, but the slight decrease with beam penetration over this range is barely outside experimental error.

The difference between the H_2O_2 yields of the neutral formate and bromide solutions is shown in Figure 7. According to generally accepted reaction mechanisms for these two systems, this difference should be equal to the OH

radical yield. The decrease with both increasing Z and beam penetration is quite clear. It is expected from track models.

Figure 8 shows the total water decomposition yield (in acid) determined using equation (4). Here the relative errors are much greater (±8%) because this is a difference between numbers of a similar magnitude. The ordinate has been split to make the graph more readable. Again, there is a slight decrease in this quantity with increasing Z and beam penetration.

The observed decrease in radical yields as the beam penetrates is quite consistent with what has been seen previously for lower Z and is what one expects qualitatively. As an ion slows down, its rate of energy loss increases and less energetic secondaries are produced. Radical recombinations are favored so the radical yields tend to decrease, as do the yields of those products which are principally derived from radicals, such as ferric ion, nitrite, and H_2O_2 from formate solutions. For different ions of the same velocity (or energy per atomic mass unit) the more highly charged ones will produce more secondary electrons of about equal energy per unit path length travelled, consequently with more likelihood of radical overlap and recombination--hence fewer radicals available for reaction with solutes.

The decrease in water decomposition yield is also expected, since radical recombination to re-form water is favored with the heavier ions, and at lower ion velocity.

The data available so far are not sufficient to calculate all the primary radical and molecular yields accurately. Other systems which will make this possible are presently under study; nevertheless, the present data are qualitatively consistent with our current ideas about the structure of heavy-ion tracks. Eventually, these data will be analyzed with the theoretical models currently being developed at LBL.

REFERENCES

1. M. Jayko, E. Christman, A. Chatterjee, and A. Appleby. Radiation chemistry of accelerated heavy particles. I. Experimental arrangements and results for the Fricke dosimeter. Radiation Research Society Meeting, San Juan, Puerto Rico, 8-12 May 1977.
2. A. Appleby, M. Jayko, E. Christman, and A. Chatterjee. Radiation chemistry of accelerated heavy particles. II. Yields of primary species in water. Radiation Research Society Meeting, San Juan, Puerto Rico, 8-12 May 1977.
3. A. Chatterjee, J. L. Magee, and M. Jayko. Radiation chemistry of accelerated heavy particles. III. Model calculations of chemical yields. Radiation Research Society Meeting, San Juan, Puerto Rico, 8-12 May 1977.
4. L. C. Northcliffe. Passage of heavy ions through matter. Annual Review of Nuclear Science 13: 67 (1963).
5. C. J. Hochanadel. Effects of cobalt gamma radiation on water and aqueous solutions. J. Phys. Chem. 56: 587-594 (1952).
6. A. O. Allen, T. W. Davis, G. Elmore, J. A. Ghormley, B. M. Haines, and C.J. Hochanadel. Oak Rdge National Laboratory, Report ORNL 130 (1949).
7. B. F. Rider and M. G. Mellon. Color determination of nitrites. Ind. Eng. Chem., Anal., Ed. 18: 96-99 (1946).
8. R. H. Schuler and A. O. Allen. Radiation chemistry studies with cyclotron beams of variable energy: yields in aerated ferrous sulfate solution. J. Amer. Chem. Soc. 79: 1565 (1957).
9. E. J. Hart, W. J. Ramler and S. R. Rocklin. Chemical yields of ionizing particles in aqueous solutions: effect of energy of protons and deuterons. Radiation Research 4: 378 (1956).

10. A. R. Anderson and E. J. Hart. Molecular product and free radical yields in the decomposition of water by protons, deuterons, and helium ions. Radiation Research 14: 689-704 (1961).

11. A. O. Allen and R. A. Holroyd. Peroxide yield in the gamma irradiation of air-saturated water. J. Amer. Chem. Soc. 77: 5852-5855 (1955).

12. Z. D. Draganic and I. G. Draganic. Studies on the formation of primary yields of hydroxyl radical and hydrated electron in the gamma-radiolysis of water. J. Phys. Chem. 77: 765-772 (1973).

Work supported by the U. S. Department of Energy.

FIGURE LEGENDS

Figure 1: The arrangement for irradiation showing target cells in their holder lined up behind the upstream ionization chamber.

Figure 2: A typical Bragg curve for carbon showing the position of the cells reported on with respect to the Bragg peak.

Figure 3: Preliminary results for the two ferrous sulfate systems: the top groups aerated; the bottom group deaerated.

Figure 4: Hydrogen peroxide yields from aerated NaBr and HCOONa.

Figure 5: Nitrite yields from the oxygen free ethanol/nitrate solutions.

Figure 6: Represents the yield of reducing free radicals that escape the spurs.

Figure 7: OH radical yield.

Figure 8: Total water decomposition in acid.

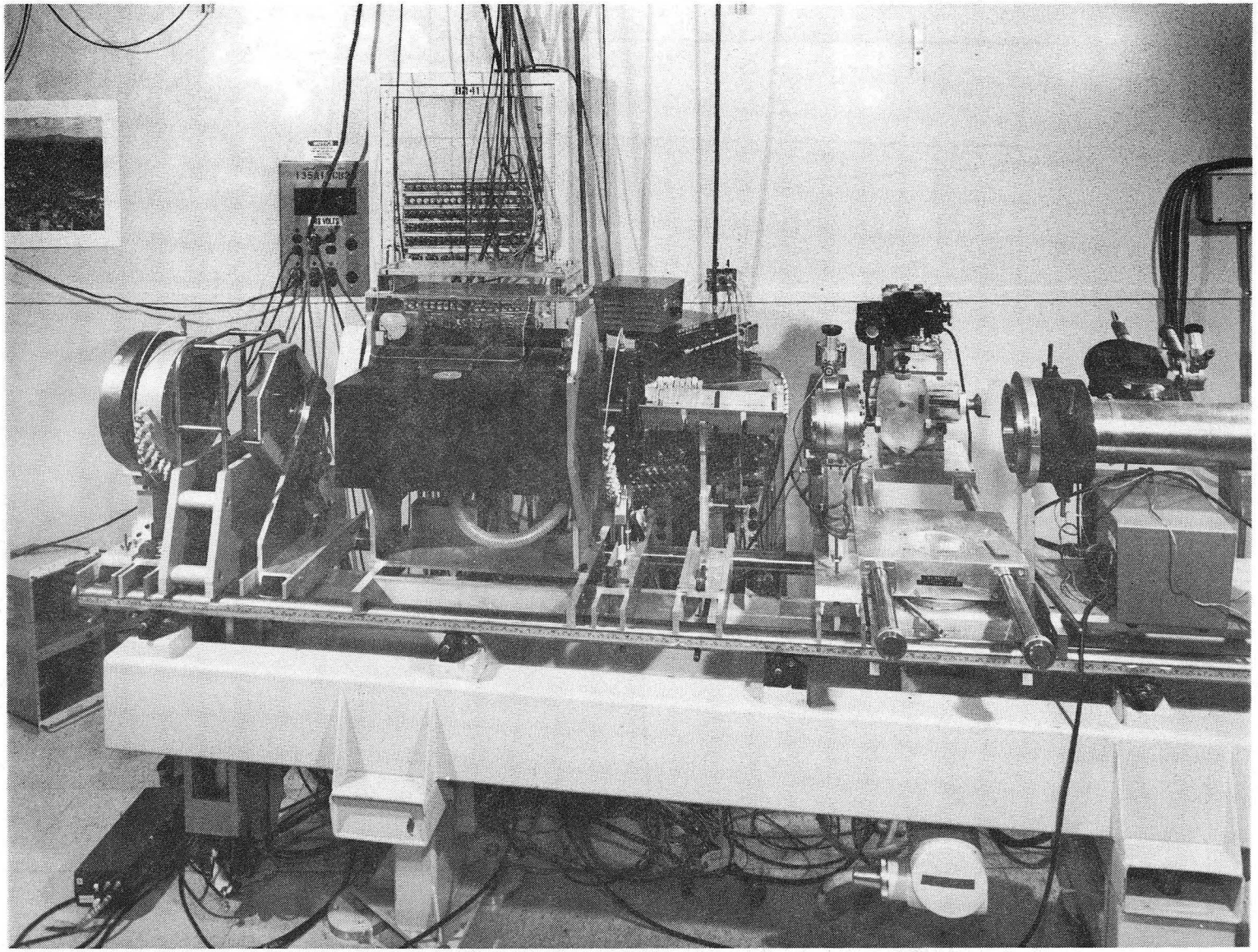

CBB 774-3668

Figure 1

FIGURE 2

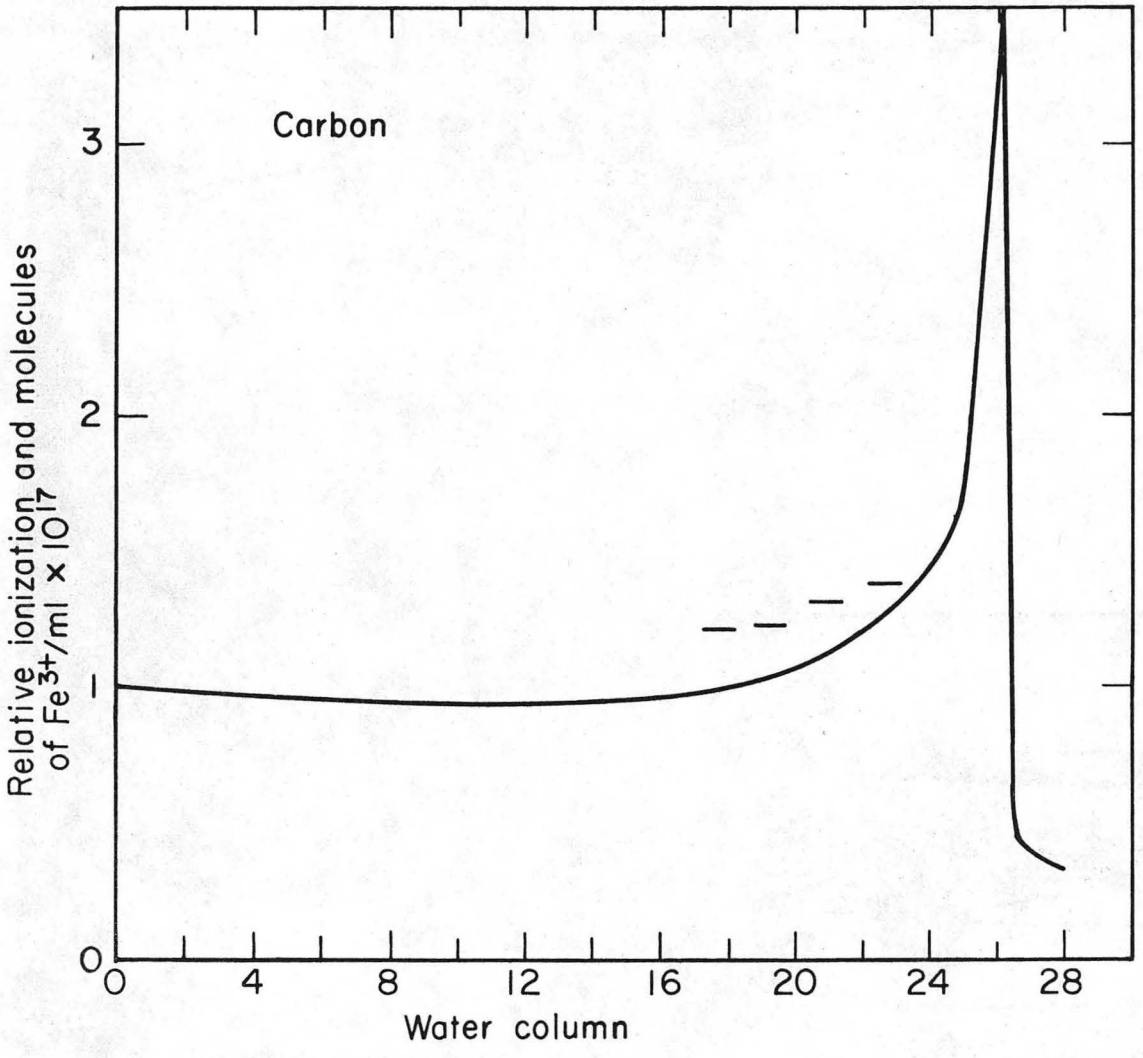

XBL775-3387A

FIGURE 3

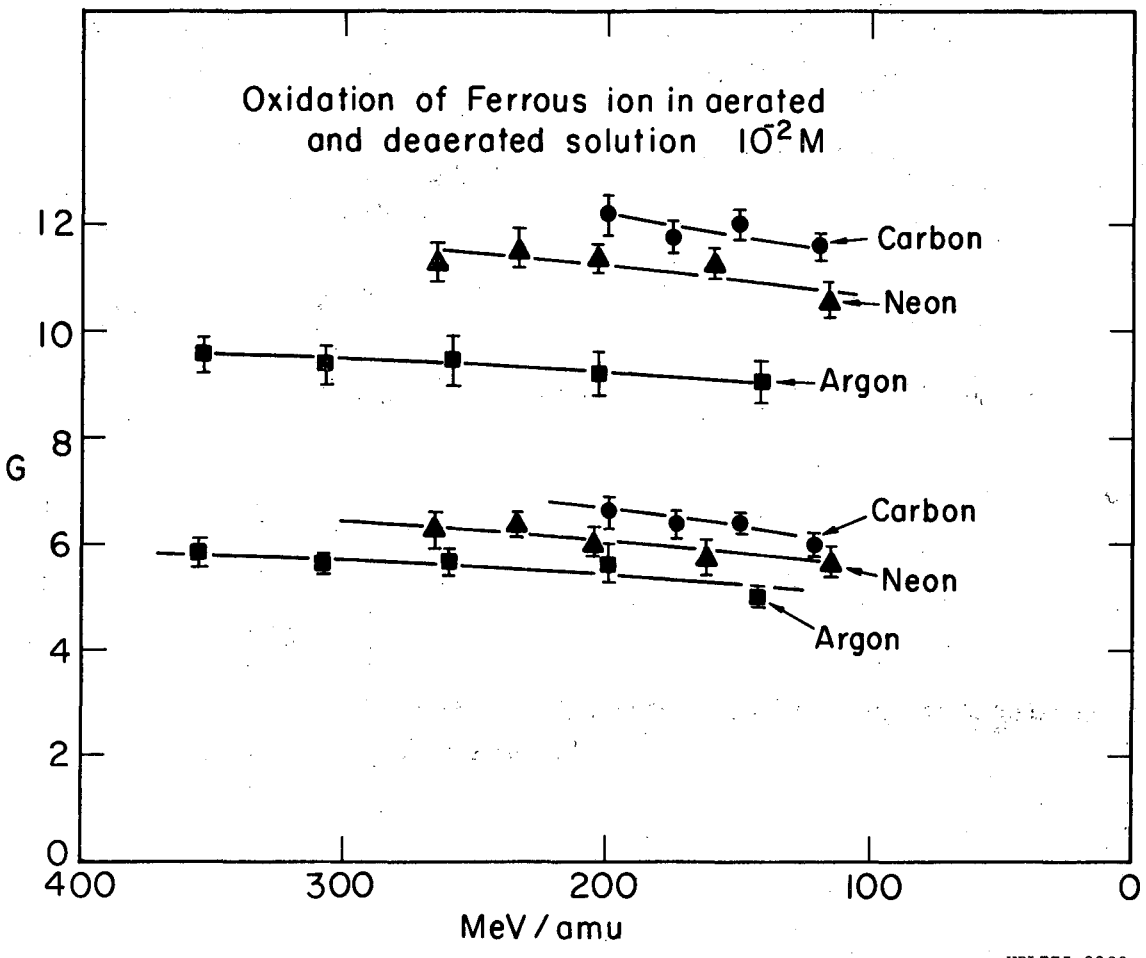
Oxidation of Ferrous ion in aerated and deaerated solution 10^{-2} M
Carbon
Neon
Argon
Carbon
Neon
Argon
G
MeV / amu
0
2
4
6
8
10
12
400
300
200
100
0
XBL775-3388

FIGURE 4

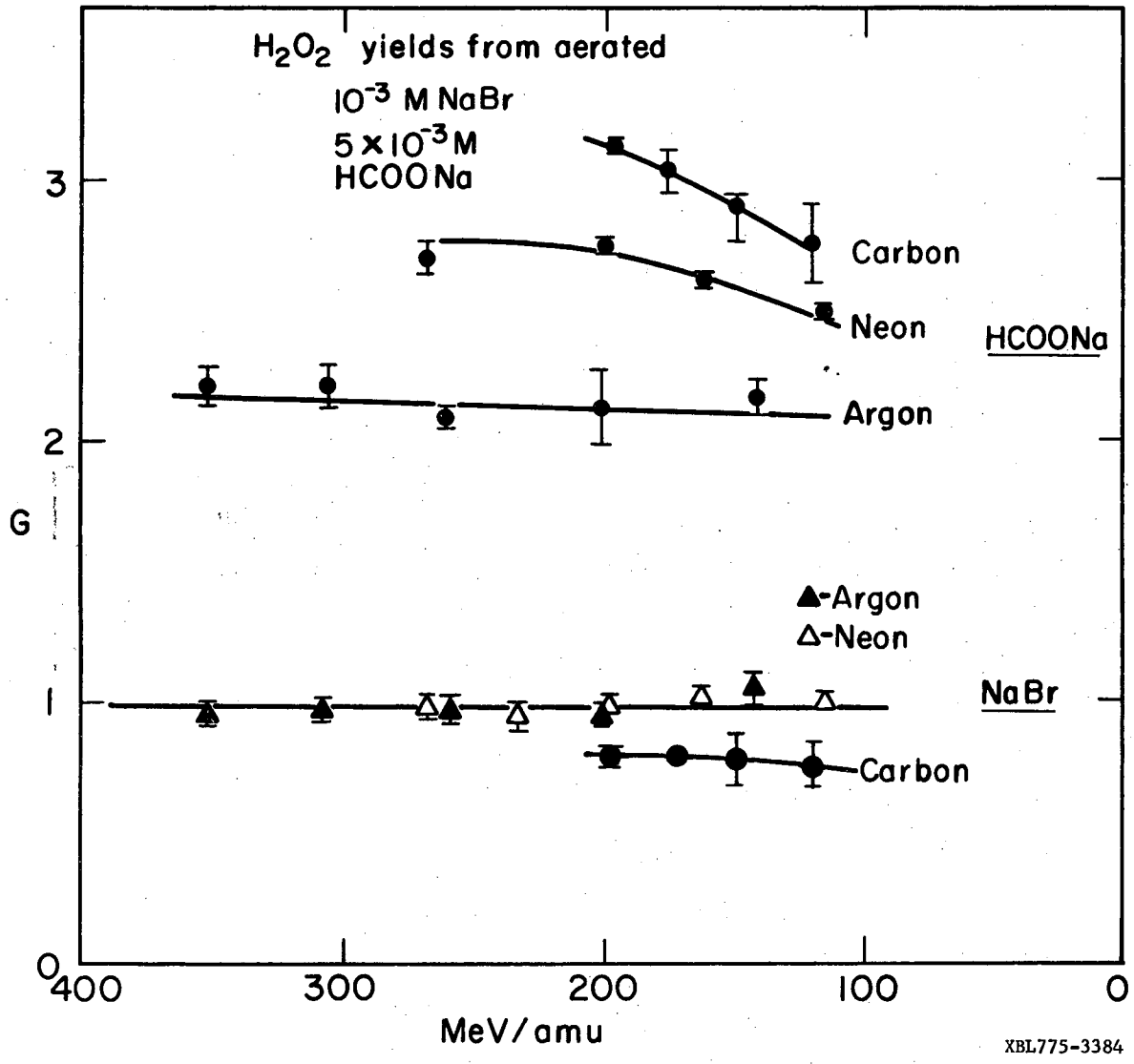
H_2O_2 yields from aerated
10^{-3} M NaBr
5×10^{-3} M
HCOONa
Carbon
Neon
HCOONa
Argon
▲-Argon
△-Neon
NaBr
Carbon
G
3
2
1
0
400
300
200
100
0
MeV/amu
XBL775-3384

FIGURE 5

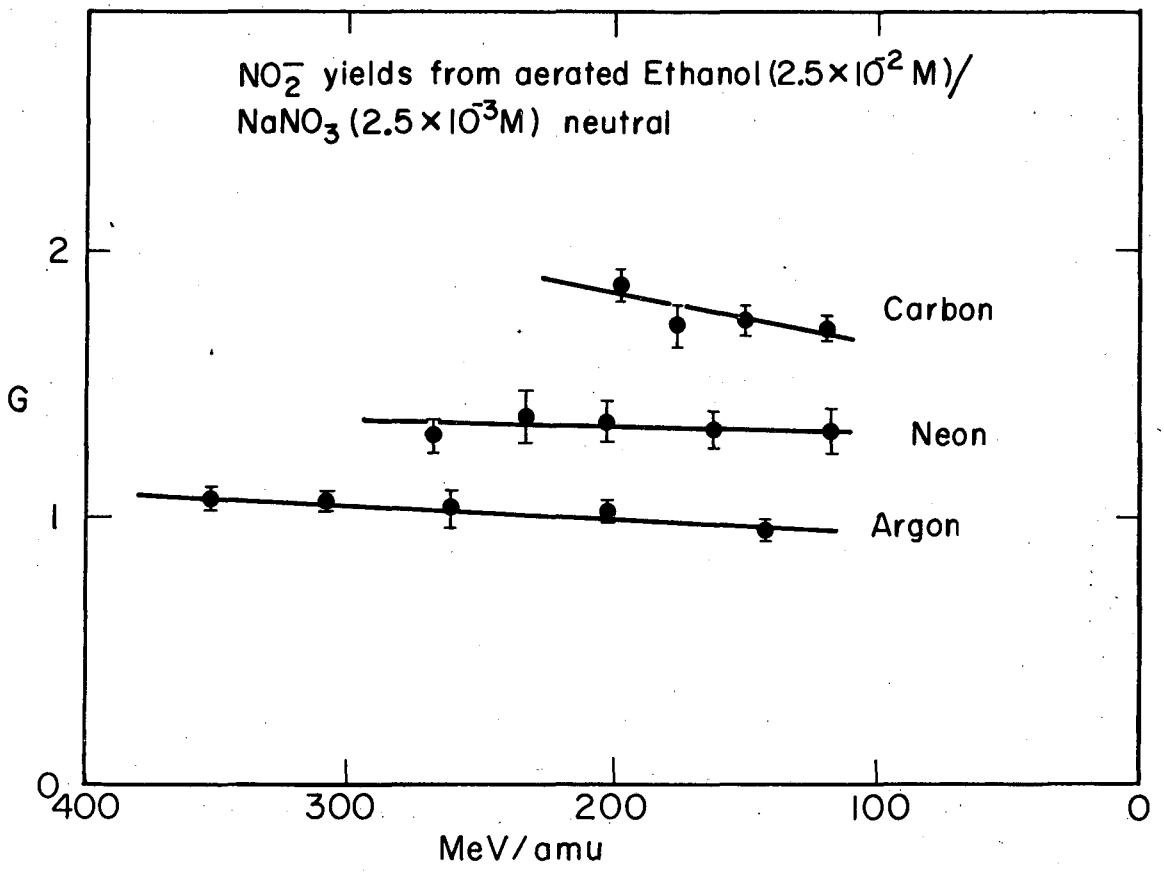

XBL775-3386

FIGURE 6

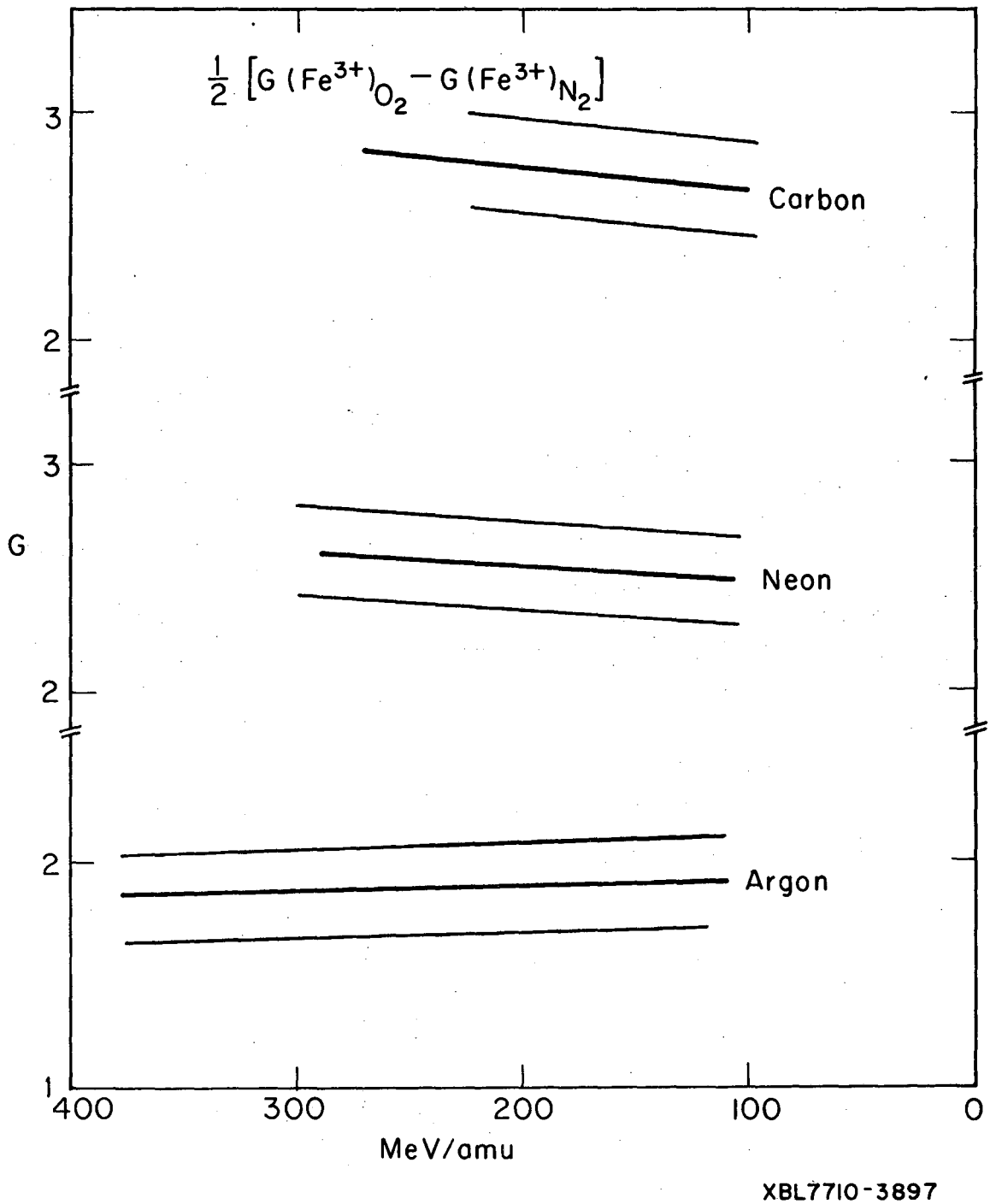

XBL7710-3897

FIGURE 7

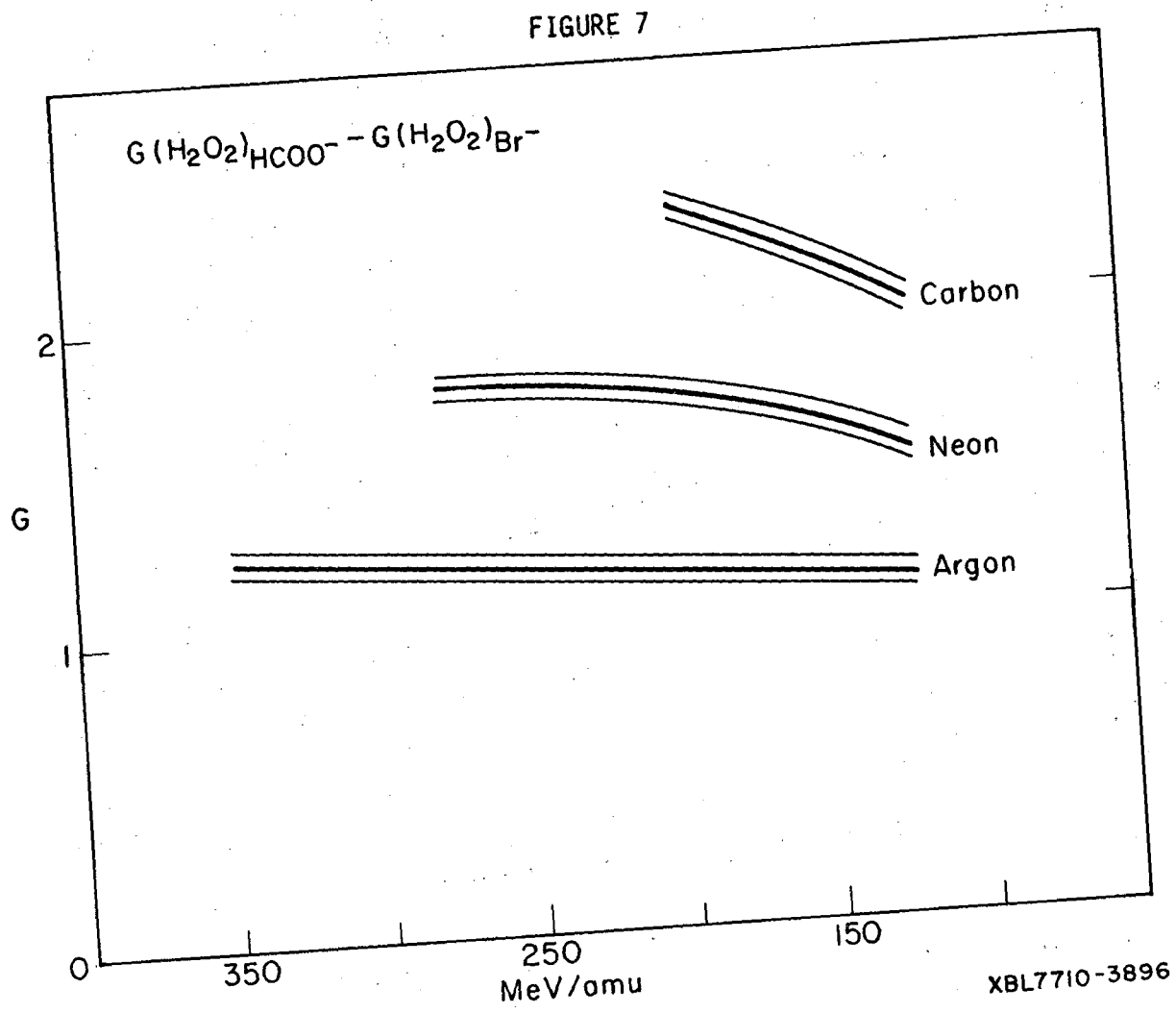
$G(H_2O_2)_{HCOO^-} - G(H_2O_2)_{Br^-}$
Carbon
Neon
Argon
G
2
1
0
350
250
150
MeV/omu
XBL7710-3896

FIGURE 8

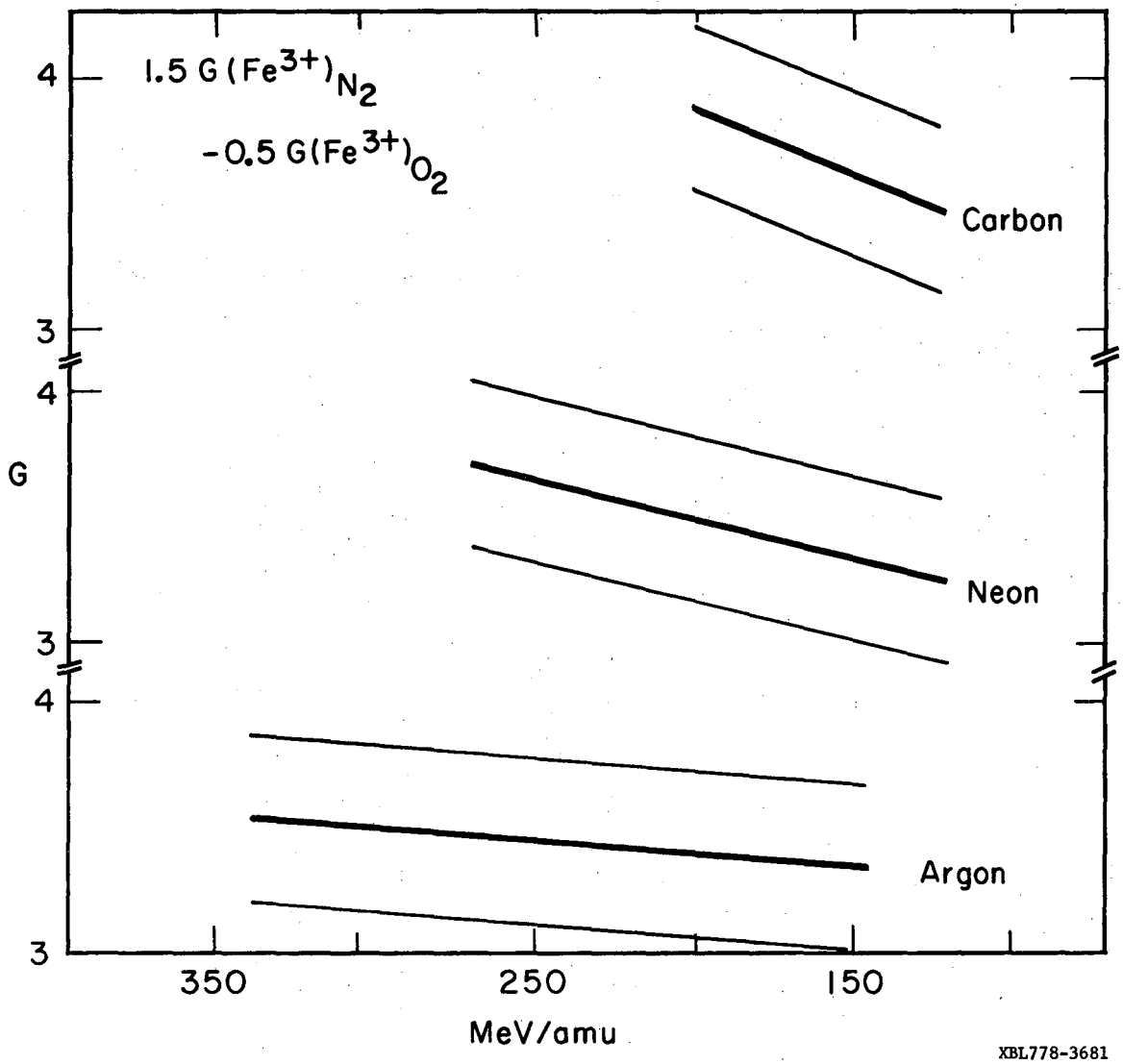
1.5 G(Fe3+)N2
-0.5 G(Fe3+)O2
Carbon
Neon
Argon
G
4
3
4
3
4
3
350
250
150
MeV/amu
XBL778-3681

This report was done with support from the Department of Energy. Any conclusions or opinions expressed in this report represent solely those of the author(s) and not necessarily those of The Regents of the University of California, the Lawrence Berkeley Laboratory or the Department of Energy.

TECHNICAL INFORMATION DEPARTMENT
LAWRENCE BERKELEY LABORATORY
UNIVERSITY OF CALIFORNIA
BERKELEY, CALIFORNIA 94720